JOURNAL OF MATERIALS SCIENCE 26 (1991) 3817–3827

Development of composite coaxial cylinder stress analysis model and its application to SiC monofilament systems

C. M. WARWICK*, T. W. CLYNE
Department of Materials Science, University of Cambridge, Pembroke Street, Cambridge, UK

An analytical model is presented allowing prediction of the principal stresses in a system composed of a set of coaxial cylinders, subject to temperature change or applied stress. The materials must exhibit transverse isotropy of stiffness and thermal expansivity. The model represents a development of an analysis published by Mikata and Taya, the modification allowing any number of component cylinders and a finite outer radius. Use of the model is illustrated by means of a series of examples involving SiC monofilaments. Application to the behaviour of composites containing many aligned fibres is demonstrated, using cylinder radii appropriate for the fibre volume fraction in the composite. It is shown by comparison with predictions from an Eshelby model that this is an acceptable approximation, preferable to the surrounding of fibre and matrix by an outer "composite" layer of infinite radius.

1. Introduction

There is considerable interest in analysing the stress state in a cylindrical rod surrounded by one or more coaxial cylindrical tubes bonded at the interfaces. The stresses of interest in such a system may arise from external tractions or from temperature changes. For example, if a fibre is to be coated with a thin protective layer before incorporation into composite material, it will be of interest to explore the generation of stresses so as to reduce the danger of cracking in this layer. Thin layers of Y_2O_3 have been found [1–3] to offer good protection in nickel, magnesium and titanium matrices, but stresses must be controlled if spallation of the coating is to be avoided. Furthermore, monofilaments produced by chemical vapour deposition (CVD) routes already have a core and sheath structure and a fabricated long fibre composite will, in many respects, exhibit behaviour which can be modelled as a single fibre surrounded by the thickness of matrix appropriate for the fibre volume fraction in the composite.

Several analytical models [4–6] have been put forward to describe the (fully elastic) stress field in a set of two or more coaxial cylinders subject to thermomechanical loading. The most complete of these, due to Mikata and Taya [6], has been formulated for a four-layer structure composed of fibre, coating, matrix and (infinite) surrounding composite. The incorporation of the surrounding composite seems physically appropriate, but it has the drawback that the axial force balance imposed as one of the boundary conditions becomes insensitive to the stresses in fibre and matrix, so that the predictions become somewhat inconsistent. Furthermore, the model is not exact in this form, because the properties taken for the composite are obtained by a weighting operation which is not rigorous. Finally, in the form presented, the model cannot be used to predict the stress state in a system, such as a single-coated fibre, having an outer free surface.

In the present paper an outline is given of how the Mikata and Taya model can be modified to allow the system to be composed of any number of concentric cylinders, with the outer surface being free. For completeness, an outline of all the mathematics involved is given in an Appendix, although this has much in common with the Mikata and Taya treatment. The new form of the model is then employed to explore several situations of practical interest involving SiC monofilaments.

2. Model development

The model is based on the imposition of various boundary conditions for stress and strain compatibility, giving a set of simultaneous equations which is solved by standard procedures. In the version described here, the stresses are induced by a uniform temperature change and/or applied stress (axial and or radial). All the component materials are assumed to exhibit transverse isotropy about the cylinder axis in stiffness and thermal expansivity. This is a good approximation for most cases of interest, although situations can be imagined for which the assumption is not valid. (An example is provided by a polycrystalline

* *Present address*: BP Research Centre, Sunbury on Thames, Middlesex, UK.

0022–2461/91 $03.00 + .12

coating exhibiting a strong texture symmetrical about the radial direction.)*

Development of the expressions allowing prediction of the final stress distribution is outlined in Appendix 1. The procedure consists essentially of ensuring equilibrium of forces and strain compatibility, so as to devise the set of simultaneous equations given at the end of Appendix 1. In the present work these were solved by a Gaussian elimination method to give the principal stresses at a preselected set of radial locations within each material. The procedure involves converting the five independent engineering constants exhibited by a transversely isotropic material to a stiffness tensor, using the matrix representation [7]. Although this falls within fairly standard elasticity theory, the relationship between engineering constants and stiffness tensor for a transversely isotropic elastic medium is outlined in Appendix 2, for ease of reference. This paper therefore contains all the equations necessary to implement the model.

3. Differential thermal contraction of free fibres

A point of interest with regard to SiC monofilaments concerns the differences between tungsten- and carbon-cored products, in terms of thermal stresses. Carbon fibre cores have been preferred by some manufacturers, although they need to be somewhat thicker than the tungsten wires and the carbon also has a larger mismatch of thermophysical properties with those of SiC than is the case for tungsten. This is apparent in Fig. 1, which compares the stress distributions† after cooling through a 1000 K temperature interval for both types of fibre, using dimensions typical of commercial products in each case. Thermophysical data used in this and following calculations are presented in Table I. Although the modulus and expansivity values of carbon fibre can vary over wide ranges, it is in general predicted that large stresses will build up in a carbon core as the temperature is changed. Cooling after fabrication should lead to axial compression, with tensile stresses in the hoop and radial directions. For a tungsten core, on the other hand, all core stresses are tensile, but the values are lower. The SiC also sustains stresses in both cases, although the significant values are confined to the interior regions near the core and even these are not much more than about 100 MPa. Again the stresses are higher for the carbon core. These internal stresses may not present a problem, and fracture of the fibre will in practice probably be more sensitive to factors such as flaws on the outer surface, but their existence should be appreciated. It may be noted that with the carbon cores, a compliant layer is sometimes created on the surface, designed partly to reduce internal stresses. For example, a thin graphitic layer with isotropic properties may be produced. The stress distribution is then changed to that shown in Fig. 2. It can be seen that this thin compliant layer is actually predicted to have very little effect on the stresses around the core.

There is also interest in the stresses generated in thin surface coatings during temperature changes. For example, yttria layers put down on to SiC monofilaments by sputter deposition should preferably be formed at high temperature, as this encourages a dense deposit [8]. Typically, deposition will be followed by a temperature decrease of several hundred degrees. As yttria has a relatively high expansivity, this gives rise to the large tensile hoop and axial stresses shown in Fig. 3. These can readily cause cracking before the coated fibre can be fabricated into a composite. (Fortunately, there is scope during sputter deposition to stimulate large compressive stresses in the deposit by the so-called "atomic peening" effect [8], which can largely offset these tensile stresses and hence stabilize the coating against spallation.)

4. Thermomechanical loading of composites

Of course, the stress distributions are quite different once the fibres have been incorporated into a composite. In the presence of a metallic matrix, accurate calculation of the stresses is hampered by the fact that the matrix is likely to undergo plastic flow and to exhibit other non-elastic behaviour such as creep.

TABLE I Properties used in calculations (typical values from various sources)

Material	Young's modulus (GPa)		Shear modulus, G_L (GPa)	Poisson's ratio		CTE ($m K^{-1}$)	
	Axial E_L	Transverse E_T		In-plane ν_{12}	Axial ν_{13}	Axial α_L	Transverse α_T
W	410	410	160	0.28	0.28	4.3	4.3
SiC	420	420	180	0.17	0.17	4.0	4.0
C fibre	200	20	20	0.25	0.20	0	10
C graphite	25	25	10	0.23	0.23	7	7
Y_2O_3	170	170	65	0.29	0.29	8.1	8.1
Ti	115	115	43	0.36	0.36	9.0	9.0

* An analytical model could be constructed in which the constituents exhibit only orthotropic symmetry (which would allow treatment of a layer with symmetry of properties about the radial direction), although this would be at the cost of increased complexity.

† Note that the radial and hoop stresses in the central core layer will always be equal to each other. This can be seen by substituting Equation A20 into Equation A18.

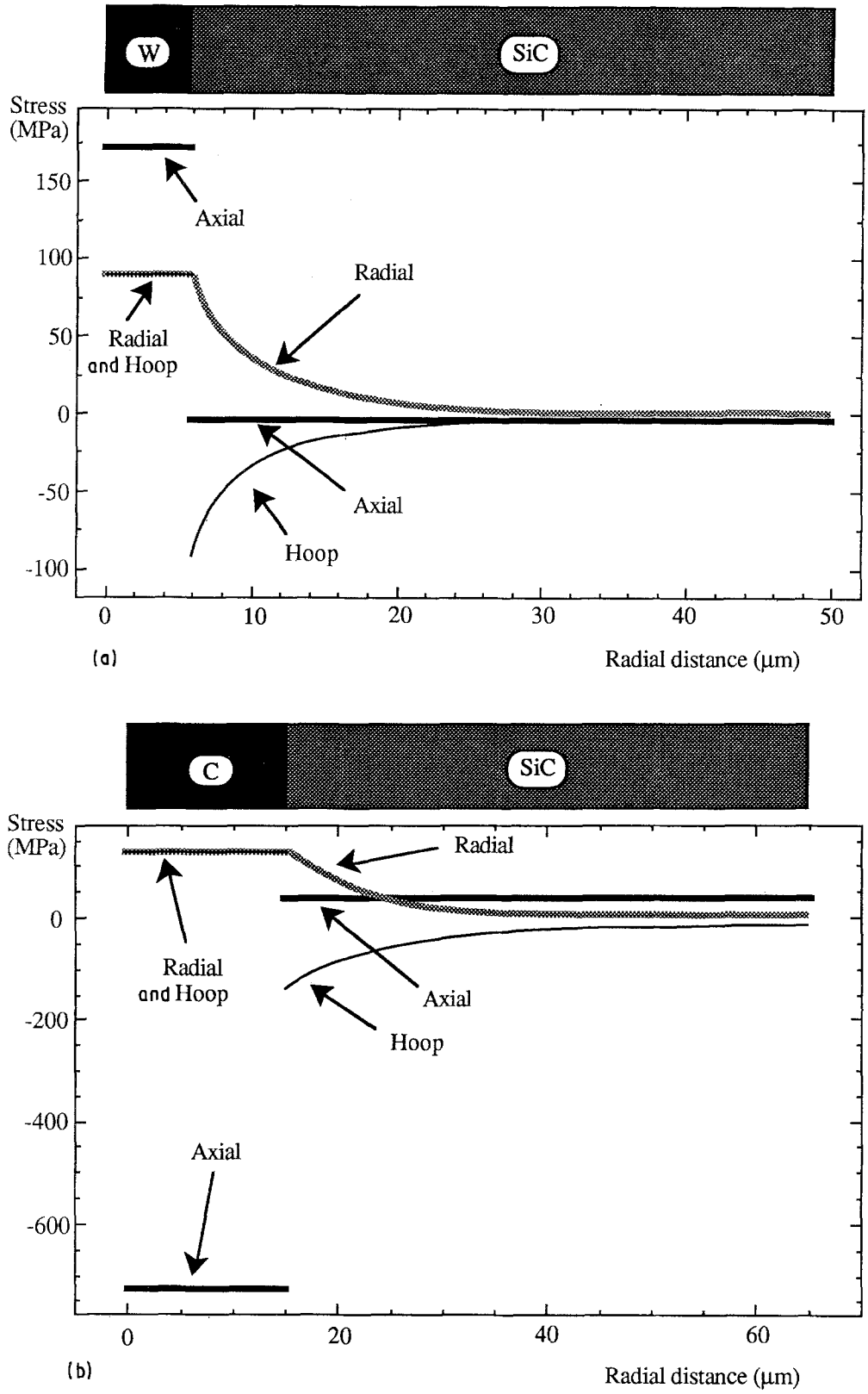

Figure 1 Comparisons between the stress distributions arising from a 1000 K temperature decrease for (a) a W-cored and (b) a C-cored SiC monofilament.

Nevertheless, a model of the current type can be useful in exploring the general nature of the stress fields, and in predicting the onset of inelastic behaviour. For example, when a SiC fibre (with the effect of the core neglected) is incorporated into a titanium matrix, so that it comprises about 35% by volume of the material, the stress state can be represented using the coaxial cylinder model with the components having the radii shown in Fig. 4. The axial and hoop stresses in the titanium at the free surface would correspond approximately to the principal in-plane stresses that would be detected at the surface of such a composite. Indeed, the values predicted here are broadly consistent with recent X-ray diffraction data [9] obtained for a titanium-based alloy reinforced with approximately this content of monofilament. That broad agreement is

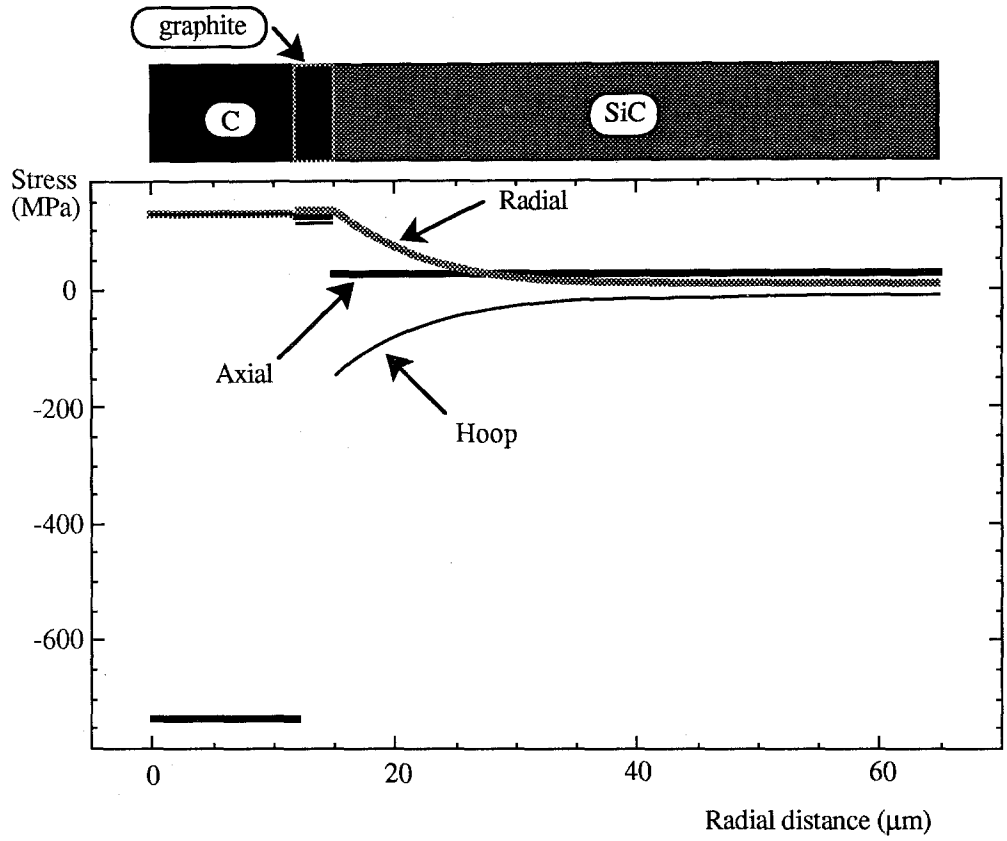

Figure 2 Stress distribution for a C-cored monofilament cooled through 1000 K with the outer 3 μm of the core composed of isotropic graphitic material.

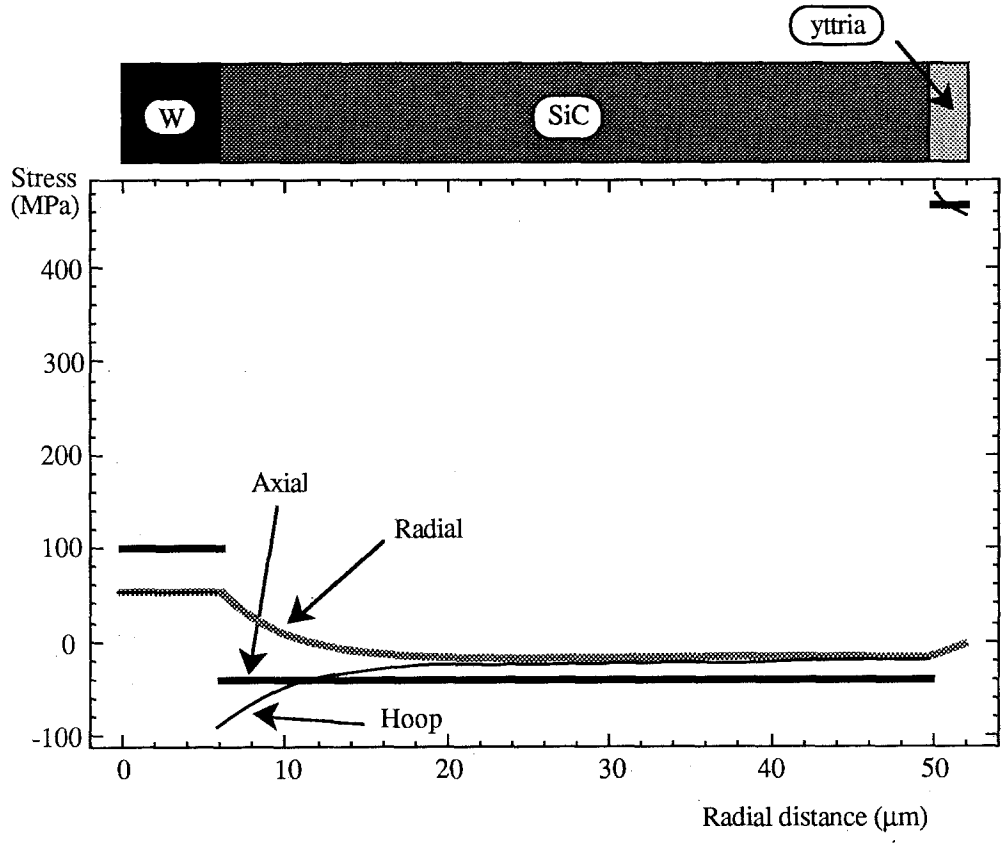

Figure 3 Stress distribution for a W-cored SiC monofilament with a 2 μm thick yttria coating, after cooling through 500 K.

obtained for a 500 K decrease, while the fabrication temperature is typically about 800–900 K above room temperature, is readily explained by high temperature stress relaxation. Note that relatively large deviatoric stresses tend to be generated in the matrix close to the fibre, with the hoop and radial stresses being the pair exhibiting the largest difference. This commonly leads to matrix plasticity adjacent to fibres in metal matrix

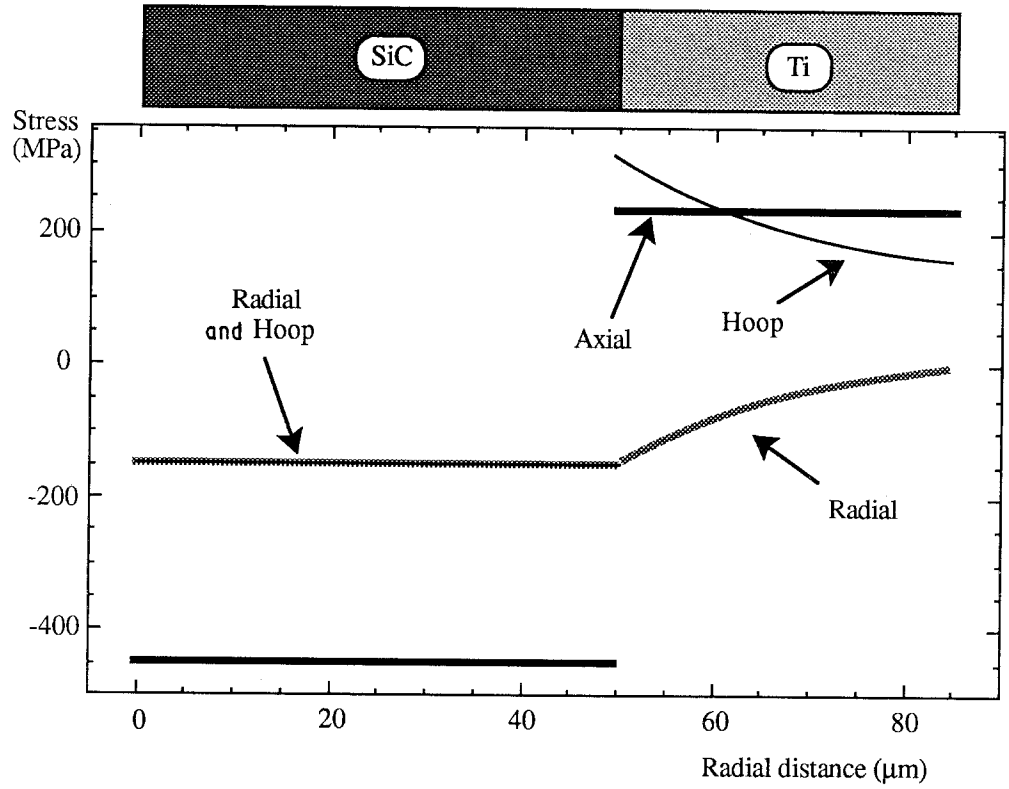

Figure 4 Stress distribution for a SiC monofilament (with no core) surrounded by a thickness of Ti matrix corresponding to a composite containing about 35% fibre, after cooling through 500 K.

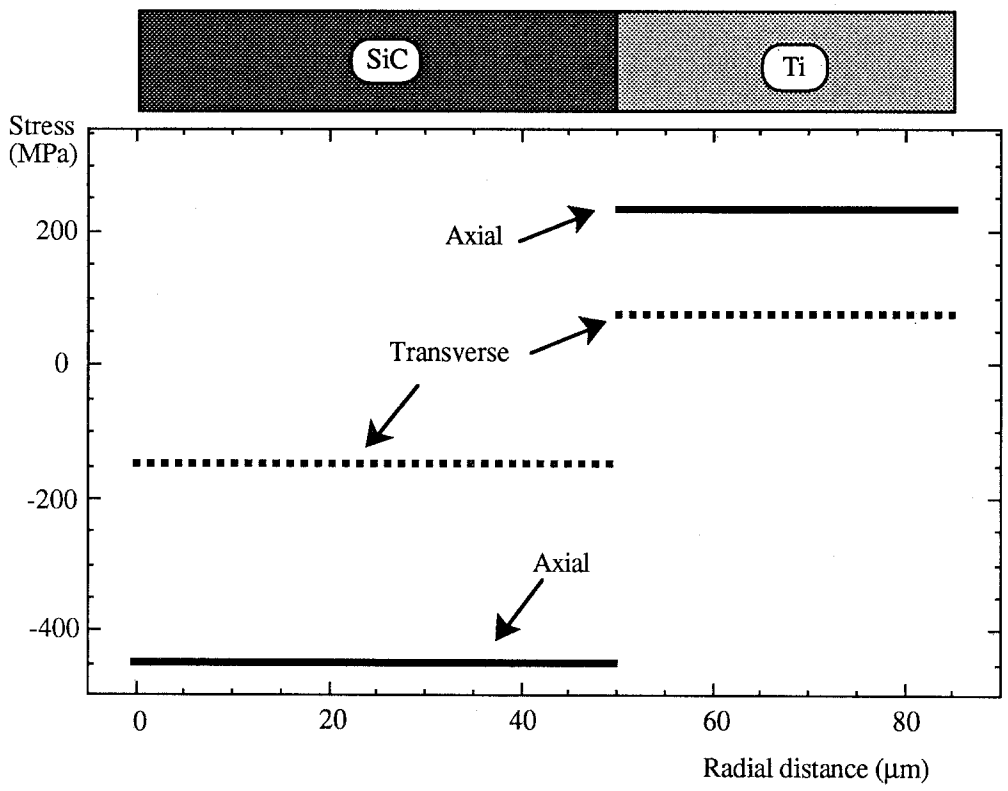

Figure 5 Predictions from the Eshelby equivalent homogeneous inclusion model for a Ti–35% SiC long-fibre composite cooled through 500 K. The stress in the fibre is predicted to be uniform, while the stresses shown for the matrix are volume-averaged values.

composites (MMCs) as a result of differential thermal contraction, with the metal predicted in this case to experience circumferential flow, but no movement in the axial direction.

Of course, the model represents an approximation for this case, in that the constraint effect of the surrounding composite material is being neglected. However, this probably makes little difference to the predictions in practice. To illustrate this, data are presented in Fig. 5 from the Eshelby equivalent homogeneous inclusion model, using the mean field approximation [10–12]. These also refer to a Ti–35 vol %

SiC long-fibre composite subjected to a 500 K temperature decrease. The stresses shown in the matrix are volume-averaged values, with the hoop and radial stresses contributing to a mean transverse value. It is clear that the stresses in the two predictions (Figs 4 and 5) show no significant discrepancies, strongly suggesting that use of the current model with a single fibre and a free surface is acceptable for representing general features of the stress distribution within an actual composite, provided that it is recognized that the predicted stress state close to the free surface will not be accurate.

Obviously, there is also interest in the response to external loading. As an example of the type of effect

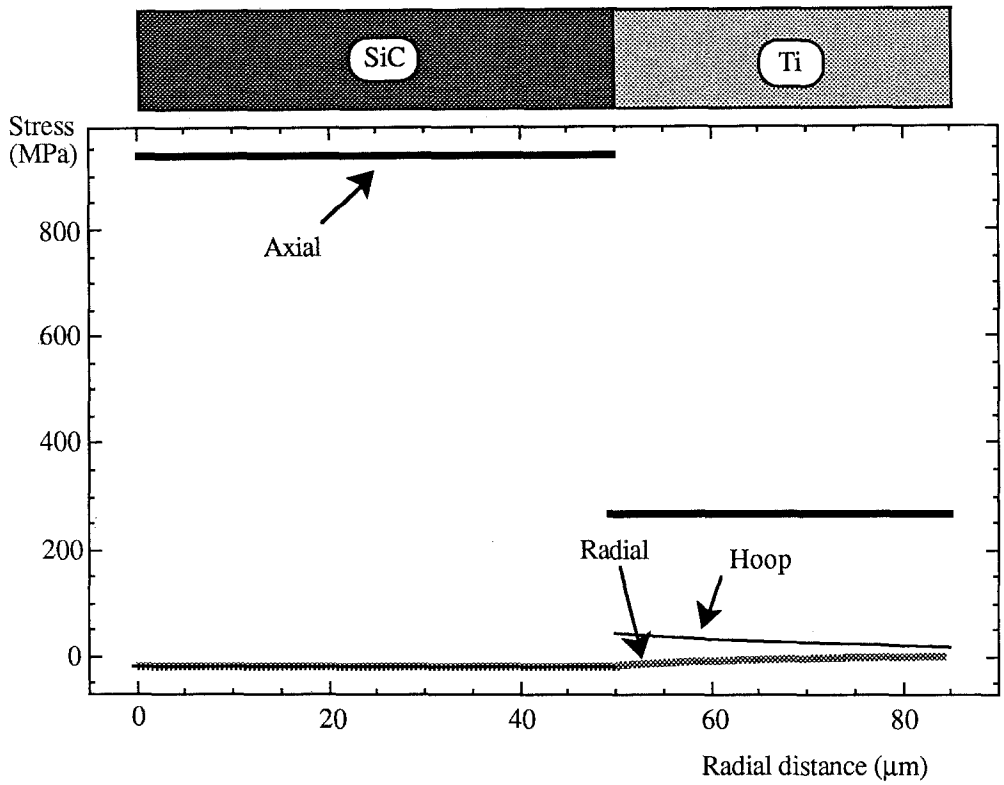

Figure 6 Predicted stress distribution for a Ti–35% SiC composite with a tensile stress of 500 MPa applied parallel to the fibre axis.

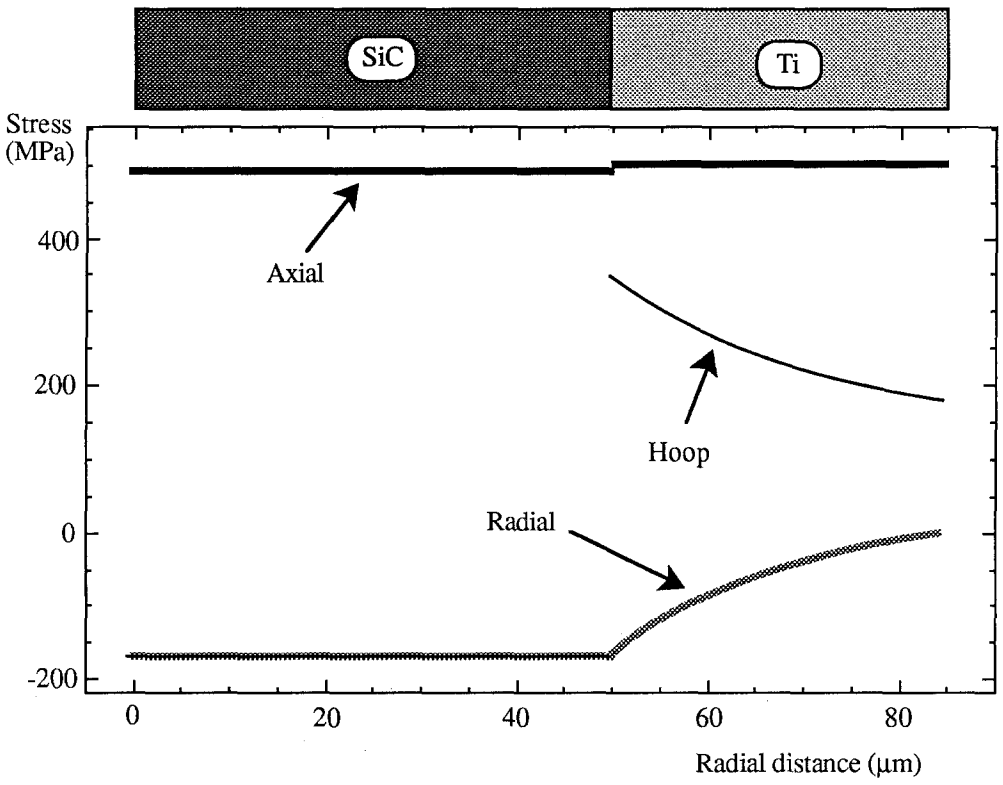

Figure 7 Predicted stress distribution for a Ti–35% SiC composite subjected to a 500 MPa applied tensile stress along the fibre axis, together with residual stresses resulting from a 500 K temperature decrease.

that can be explored, Figs 6 and 7 show predicted distributions for an SiC fibre in a titanium matrix, subjected to a 500 MPa tensile stress along the fibre axis, with and without the internal stresses associated with a 500 K temperature decrease. In the absence of thermal residual stresses, the fibre carries much of the axial load and all the stresses in the matrix are relatively low. However, the thermal stresses cause significant changes, transferring much of the axial load to the matrix, which must now sustain large deviatoric stresses, particularly in the vicinity of the fibre. Evidently, close attention must be paid to thermomechanical history with such composites.

5. Conclusion

An analytical model has been outlined for prediction of the stress distribution within a composite system composed of a number of coaxial cylinders, perfectly bonded at the mating interfaces, as a result of subjecting this system to a uniform temperature change and/or an applied stress in the axial and/or radial directions. The model, which is mathematically rigorous, is a development of an analysis published by Mikata and Taya. The version presented here is more general, in that it allows any number of component cylinders in the model and is not restricted to having an outer layer which is infinitely thick.

A number of predictions from the model have been presented, using SiC monofilaments subjected to different situations. It has been shown, for example, that cooling of CVD monofilaments from the fabrication temperature can lead to large compressive axial stresses in a carbon core, while significant hoop and radial stresses appear in the SiC near the interface for both tungsten and carbon cores. Attention has also been drawn to the difficulties of avoiding large tensile stresses, and hence cracking, in coatings deposited (usually at elevated temperature) on the free surface of fibres. Such coatings may be applied for a variety of purposes and in many cases have a higher thermal expansivity than the fibre, leading to large tensile hoop and axial stresses on cooling.

Finally, the model has been applied to predict the stress state within aligned continuous fibre composites, by choosing cylinder radii appropriate for the fibre volume fraction. This has been used, for example, to show that deviatoric stresses sufficient to cause matrix yielding are easily generated during post-fabrication cooling of metal matrix composites, particularly in the region near the fibre. The predicted stress state near the free surface of the outer cylinder will obviously not correspond to that anywhere within the real composite, but a comparison with predictions obtained using the Eshelby equivalent homogeneous inclusion with a mean field approximation has shown that the predicted average stresses in both constituents are correct in the current model, and it seems advisable not to use an outer "composite" layer of infinite thickness. The stress state in the matrix near the fibres is probably well represented by the proposed model, and it is only near the free surface that the predictions may deviate somewhat from the real situation. In practice, of course, plastic flow or other relaxation processes may cause the stress distribution in many composites to differ considerably from that predicted on the basis of elastic behaviour.

Acknowledgements

Financial support for one of us (CMW) was provided by BP plc. The authors are grateful for the collaboration and help offered by staff at BP Research Centre, Sunbury on Thames, particularly Dr C.W. Brown and Mr J. Robertson.

Appendix 1. Stresses in concentric cylinders

To find the stress distribution in a system of N concentric cylinders, after a temperature change, ΔT, with applied radial and longitudinal stresses, σ_{0r} and σ_{0z}.

r, θ, z	Radial, tangential and longitudinal coordinates
$\boldsymbol{C}^{(n)}$	Stiffness of layer n
$\boldsymbol{\sigma}^{(n)}$	Stress in layer n
$\boldsymbol{e}^{(n)}$	Strain in layer n
$\alpha_T^{(n)}$	Transverse coefficient of thermal expansion (CTE) of layer n
$\alpha_L^{(n)}$	Longitudinal CTE of layer n
T_n	Temperature difference in layer $n = \Delta T$
$u_n(r)$	Radial displacement in layer n
$w_n(z)$	Longitudinal displacement in layer n
u_r, u_θ, u_z	Radial, tangential and longitudinal displacements
l_n, $\beta_1^{(n)}$, $\beta_3^{(n)}$	Parameters for layer n derived from stiffness and CTE
r_n	Outer radius of layer n
A_n, B_n	Integration constants
E_n, F_n	Integration constants

The stress equilibrium relations in cylindrical coordinates are

$$\frac{1}{r}\frac{\partial}{\partial r}(r\sigma_{rr}^{(n)}) + \frac{1}{r}\frac{\partial \sigma_{r\theta}^{(n)}}{\partial \theta} + \frac{\partial \sigma_{rz}^{(n)}}{\partial z} - \frac{\sigma_{\theta\theta}^{(n)}}{r} = 0 \quad \text{(A1a)}$$

$$\frac{1}{r^2}\frac{\partial}{\partial r}(r^2\sigma_{\theta r}^{(n)}) + \frac{1}{r}\frac{\partial \sigma_{\theta\theta}^{(n)}}{\partial \theta} + \frac{\partial \sigma_{\theta z}^{(n)}}{\partial z} = 0 \quad \text{(A1b)}$$

$$\frac{1}{r}\frac{\partial}{\partial r}(r\sigma_{zr}^{(n)}) + \frac{1}{r}\frac{\partial \sigma_{z\theta}^{(n)}}{\partial \theta} + \frac{\partial \sigma_{zz}^{(n)}}{\partial z} = 0 \quad \text{(A1c)}$$

The stresses are given by

$$\sigma_{rr}^{(n)} = C_{11}^{(n)} e_{rr}^{(n)} + C_{12}^{(n)} e_{\theta\theta}^{(n)} + C_{13}^{(n)} e_{zz}^{(n)} - \beta_1^{(n)} T_n \quad \text{(A2a)}$$

$$\sigma_{\theta\theta}^{(n)} = C_{12}^{(n)} e_{rr}^{(n)} + C_{11}^{(n)} e_{\theta\theta}^{(n)} + C_{13}^{(n)} e_{zz}^{(n)} - \beta_1^{(n)} T_n \quad \text{(A2b)}$$

$$\sigma_{zz}^{(n)} = C_{13}^{(n)} e_{rr}^{(n)} + C_{13}^{(n)} e_{\theta\theta}^{(n)} + C_{33}^{(n)} e_{zz}^{(n)} - \beta_3^{(n)} T_n \quad \text{(A2c)}$$

$$\sigma_{rz}^{(n)} = 2C_{44}^{(n)} e_{rz}^{(n)} \quad \text{(A2d)}$$

$$\sigma_{\theta z}^{(n)} = 2C_{44}^{(n)} e_{\theta z}^{(n)} \quad \text{(A2e)}$$

$$\sigma_{r\theta}^{(n)} = (C_{11}^{(n)} - C_{12}^{(n)}) e_{r\theta}^{(n)} \quad \text{(A2f)}$$

where

$$\beta_1^{(n)} = (C_{11}^{(n)} + C_{12}^{(n)})\alpha_T^{(n)} + C_{13}^{(n)}\alpha_L^{(n)} \quad \text{(A3a)}$$

$$\beta_3^{(n)} = 2C_{12}^{(n)}\alpha_T^{(n)} + C_{33}^{(n)}\alpha_L^{(n)} \quad \text{(A3b)}$$

In terms of displacement, u, the strains are given by

$$e_{rr}^{(n)} = \frac{\partial u_r^{(n)}}{\partial r} \quad \text{(A4a)}$$

$$e_{\theta\theta}^{(n)} = \frac{1}{r}\frac{\partial u_\theta^{(n)}}{\partial\theta} + \frac{u_r^{(n)}}{r} \quad \text{(A4b)}$$

$$e_{zz}^{(n)} = \frac{\partial u_z^{(n)}}{\partial z} \quad \text{(A4c)}$$

$$e_{rz}^{(n)} = \frac{1}{2}\left(\frac{\partial u_z^{(n)}}{\partial r} + \frac{\partial u_r^{(n)}}{\partial z}\right) \quad \text{(A4d)}$$

$$e_{\theta z}^{(n)} = \frac{1}{2}\left(\frac{\partial u_\theta^{(n)}}{\partial z} + \frac{1}{r}\frac{\partial u_z^{(n)}}{\partial\theta}\right) \quad \text{(A4e)}$$

$$e_{r\theta}^{(n)} = \frac{1}{2}\left(\frac{1}{r}\frac{\partial u_r^{(n)}}{\partial\theta} + \frac{\partial u_\theta^{(n)}}{\partial r} - \frac{u_\theta^{(n)}}{r}\right) \quad \text{(A4f)}$$

Radial symmetry, therefore

$$u_r^{(n)} = u_n(r) \quad \text{(A5a)}$$

$$u_\theta^{(n)} = 0 \quad \text{(A5b)}$$

$$u_z^{(n)} = w_n(z) \quad \text{(A5c)}$$

giving:

$$e_{rr}^{(n)} = \frac{\partial u_n}{\partial r} \quad \text{(A6a)}$$

$$e_{\theta\theta}^{(n)} = \frac{u_n}{r} \quad \text{(A6b)}$$

$$e_{zz}^{(n)} = \frac{\partial w_n}{\partial z} \quad \text{(A6c)}$$

$$e_{rz}^{(n)} = e_{\theta z}^{(n)} = e_{r\theta}^{(n)} = 0 \quad \text{(A6d)}$$

which, on substitution into Equations A2 gives

$$\sigma_{rr}^{(n)} = C_{11}^{(n)}\frac{\partial u_n}{\partial r} + C_{12}^{(n)}\frac{u_n}{r} + C_{13}^{(n)}\frac{\partial w_n}{\partial z} - \beta_1^{(n)}T_n \quad \text{(A7a)}$$

$$\sigma_{\theta\theta}^{(n)} = C_{12}^{(n)}\frac{\partial u_n}{\partial r} + C_{11}^{(n)}\frac{u_n}{r} + C_{13}^{(n)}\frac{\partial w_n}{\partial z} - \beta_1^{(n)}T_n \quad \text{(A7b)}$$

$$\sigma_{zz}^{(n)} = C_{13}^{(n)}\frac{\partial u_n}{\partial r} + C_{13}^{(n)}\frac{u_n}{r} + C_{33}^{(n)}\frac{\partial w_n}{\partial z} - \beta_3^{(n)}T_n \quad \text{(A7c)}$$

$$\sigma_{rz}^{(n)} = 0 \quad \text{(A7d)}$$

$$\sigma_{\theta z}^{(n)} = 0 \quad \text{(A7e)}$$

$$\sigma_{r\theta}^{(n)} = 0 \quad \text{(A7f)}$$

Substitution into Equations A1 gives the differential equations

$$\frac{d^2u_n}{dr^2} + \frac{1}{r}\frac{du_n}{dr} - \frac{u_n}{r^2} = l_n\frac{dT_n}{dr} \quad \text{(A8a)}$$

$$\frac{d^2w_n}{dz^2} = 0 \quad \text{(A8b)}$$

where

$$l_n = \frac{\beta_1^{(n)}}{C_{11}^{(n)}} \quad \text{(A9)}$$

Because we are considering a uniform temperature change

$$\frac{dT_n}{dr} = 0 \quad \text{(A10)}$$

So Equations A8 are solved by

$$u_n(r) = A_n r + \frac{B_n}{r} \quad \text{(A11)}$$

$$w_n(z) = E_n z + F_n \quad \text{(A12)}$$

The boundary conditions imposed are

$$\sigma_{rr}^{(n)} = \sigma_{0r} \quad \text{at } r = r_N \quad \text{(A13)}$$

$$u_n = u_{n+1},\ w_n = w_{n+1},\ \sigma_{rr}^{(n)} = \sigma_{rr}^{(n+1)} \quad \text{at } r = r_n \quad \text{(A14)}$$

for $n = 1$ to $N-1$

and

$$\sum_{n=1}^{N}\int_{r_{n-1}}^{r_n}\sigma_{zz}^{(n)} r\,dr = \int_0^{r_N}\sigma_{0z} r\,dr \quad \text{with } r_0 = 0 \quad \text{(A15)}$$

Without loss of generality

$$F_1 = F_2 = \cdots = F_i = \cdots = F_{N-1} = F_N = 0 \quad \text{(A16)}$$

Equation A14 leads to

$$E_1 = E_2 = \cdots = E_i = \cdots = E_{N-1} = E_N = E \quad \text{(A17)}$$

Substituting Equations A11 and A12 back into Equation A7 gives

$$\sigma_{rr} = C_{11}^{(n)}\left[A_n - \frac{B_n}{r^2}\right] + C_{12}^{(n)}\left[A_n + \frac{B_n}{r^2}\right] + C_{13}^{(n)}E - \beta_1^{(n)}\Delta T \quad \text{(A18a)}$$

$$\sigma_{\theta\theta} = C_{11}^{(n)}\left[A_n + \frac{B_n}{r^2}\right] + C_{12}^{(n)}\left[A_n - \frac{B_n}{r^2}\right] + C_{13}^{(n)}E - \beta_1^{(n)}\Delta T \quad \text{(A18b)}$$

$$\sigma_{zz} = 2C_{13}^{(n)}A_n + C_{33}^{(n)}E - \beta_3^{(n)}\Delta T \quad \text{(A18c)}$$

Because

$$T_n = \Delta T \quad \text{(A19)}$$

$u_1(0)$ must remain finite

$$B_1 = 0 \quad \text{(A20)}$$

Now there are $2N$ simultaneous equations to set up

$$(b_1 \quad b_2 \quad \cdots \quad b_{2N}) = \begin{pmatrix} a_{1,1} & a_{1,2} & \cdots & a_{1,N} & a_{1,N+1} & a_{1,N+2} & \cdots & a_{1,2N-1} & a_{1,2N} \\ a_{1,1} & a_{1,2} & \cdots & a_{1,N} & a_{1,N+1} & a_{1,N+2} & \cdots & a_{1,2N-1} & a_{1,2N} \\ \cdots & \cdots & \cdots & \cdots & \cdots & \cdots & \cdots & \cdots & \cdots \\ a_{1,1} & a_{1,2} & \cdots & a_{1,N} & a_{1,N+1} & a_{1,N+2} & \cdots & a_{1,2N-1} & a_{1,2N} \end{pmatrix} \begin{pmatrix} A_1 \\ A_2 \\ \\ A_N \\ B_2 \\ B_3 \\ \\ B_N \\ E \end{pmatrix} \quad \text{(A21a)}$$

i.e each equation is of the form

$$\sum_{i=1}^{N} a_{k,i}A_i + \sum_{j=2}^{N} a_{k,(n-1)+j}B_j + a_{k,2N}E = b_k$$

$$\text{for } k = 1 \text{ to } 2N \tag{A21b}$$

Starting with Equation A14 gives $N-1$ equations

$$\text{for } k = 1 \text{ to } N-1$$

$$A_k r_k - A_{k+1} r_k + \frac{B_k}{r_k} - \frac{B_{k+1}}{r_k} = 0 \tag{A22}$$

$$a_{k,k} = r_k \tag{A23a}$$

$$a_{k,k+1} = -r_k \tag{A23b}$$

$$a_{k,N+k-1} = \frac{1}{r_k} \tag{A23c}$$

$$a_{k,N+k} = -\frac{1}{r_k} \tag{A23d}$$

$$b_k = 0 \tag{A23e}$$

Then Equation A14 gives another $N-1$ equations

$$\text{for } i = 1 \text{ to } N-1,\ k = N+i$$

$$A_i[C_{11}^{(i)} + C_{12}^{(i)}] - A_{i+1}[C_{11}^{(i+1)} + C_{12}^{(i+1)}] + B_i\left[\frac{C_{12}^{(i)} - C_{11}^{(i)}}{r_i^2}\right] - B_{i+1}\left[\frac{C_{12}^{(i+1)} - C_{11}^{(i+1)}}{r_i^2}\right] + E[C_{13}^{(i)} - C_{13}^{(i+1)}] = \Delta T(\beta_1^{(i)} - \beta_1^{(i+1)}) \tag{A24}$$

$$a_{k,i} = [C_{11}^{(i)} + C_{12}^{(i)}] \tag{A25a}$$

$$a_{k,i+1} = -[C_{11}^{(i+1)} + C_{12}^{(i+1)}] \tag{A25b}$$

$$a_{k,N+i-1} = \left[\frac{C_{12}^{(i)} - C_{11}^{(i)}}{r_i^2}\right] \tag{A25c}$$

$$a_{k,N+i} = -\left[\frac{C_{12}^{(i+1)} - C_{11}^{(i+1)}}{r_i^2}\right] \tag{A25d}$$

$$a_{k,2N} = [C_{13}^{(i)} - C_{13}^{(i+1)}] \tag{A25e}$$

$$b_k = \Delta T(\beta_1^{(i)} - \beta_1^{(i+1)}) \tag{A25f}$$

Equation A13 yields one more equation

$$A_N[C_{11}^{(N)} + C_{12}^{(N)}] + B_N\left[\frac{C_{12}^{(N)} - C_{11}^{(N)}}{r_i^2}\right] + EC_{13}^{(N)} = \sigma_{0r} + \beta_1^{(N)}\Delta T \tag{A26}$$

$$a_{N,N} = [C_{11}^{(N)} + C_{12}^{(N)}] \tag{A27a}$$

$$a_{N,2N-1} = \left[\frac{C_{12}^{(N)} - C_{11}^{(N)}}{r_i^2}\right] \tag{A27b}$$

$$a_{N,2N} = C_{13}^{(N)} \tag{A27c}$$

$$b_N = \sigma_{0r} + \beta_1^{(N)}\Delta T \tag{A27d}$$

And Equation A15 gives the final simultaneous equation

$$\sum_{i=1}^{N} [2C_{13}^{(i)}A_i + C_{33}^{(i)}E - \beta_3^{(i)}\Delta T](r_i^2 - r_{i-1}^2) = \sigma_{0z}r_N^2 \tag{A28}$$

$$\begin{aligned}\sigma_{0z}r_N^2 + \Delta T\sum_{i=1}^{N}\beta_3^{(i)}(r_i^2 - r_{i-1}^2) &= 2A_1C_{13}^{(1)}r_1^2 \\ &+ 2A_2C_{13}^{(2)}(r_2^2 - r_1^2) \\ &\vdots \\ &+ 2A_iC_{13}^{(i)}(r_i^2 - r_{i-1}^2) \\ &\vdots \\ &+ 2A_{N-1}C_{13}^{(N-1)}(r_{N-1}^2 - r_{N-2}^2) \\ &+ 2A_NC_{13}^{(N)}(r_N^2 - r_{N-1}^2) \\ &+ E\sum_{i=1}^{N}C_{33}^{(i)}(r_i^2 - r_{i-1}^2)\end{aligned} \tag{A29}$$

$$a_{2N,1} = 2C_{13}^{(1)}r_1^2 \tag{A30a}$$

$$a_{2N,2} = 2C_{13}^{(2)}(r_2^2 - r_1^2) \tag{A30b}$$

$$a_{2N,i} = 2C_{13}^{(i)}(r_i^2 - r_{i-1}^2) \tag{A30c}$$

$$a_{2N,N-1} = 2C_{13}^{(N-1)}(r_{N-1}^2 - r_{N-2}^2) \tag{A30d}$$

$$a_{2N,N} = 2C_{13}^{(n)}(r_N^2 - r_{N-1}^2) \tag{A30e}$$

$$a_{2N,2N} = \sum_{i=1}^{N}C_{33}^{(i)}(r_i^2 - r_{i-1}^2) \tag{A30f}$$

$$b_{2N} = \sigma_{0z}r_N^2 + \Delta T\sum_{i=1}^{N}\beta_3^{(i)}(r_i^2 - r_{i-1}^2) \tag{A30g}$$

All other values of $a_{k,j}$ are set to zero and the simultaneous equations may then be solved to give the values A_n, B_n and E which may be substituted into Equation A18 to give the stresses.

Appendix 2. The transversely isotropic stiffness tensor

The engineering elastic constants for a transversely isotropic material are:

E_T = in-plane Young's modulus
E_L = longitudinal Young's modulus
ν_{12} = in-plane Poisson's ratio
ν_{13} = longitudinal Poisson's ratio
G_L = longitudinal shear modulus

$$\nu_{31} = \nu_{13}\frac{E_T}{E_L}$$

$$G_T = \frac{E_T}{2(1+\nu_{12})}$$

Let r, θ, z = cylindrical coordinates
σ = stress
e = strain

Let

$$\sigma_{rr} = \sigma_1 \tag{A31a}$$

$$\sigma_{\theta\theta} = \sigma_2 \tag{A31b}$$

$$\sigma_{zz} = \sigma_3 \tag{A31c}$$

$$\sigma_{\theta z} = \sigma_4 \tag{A31d}$$

$$\sigma_{rz} = \sigma_5 \quad \text{(A31e)}$$

$$\sigma_{r\theta} = \sigma_6 \quad \text{(A31f)}$$

and

$$e_{rr} = e_1 \quad \text{(A32a)}$$

$$e_{\theta\theta} = e_2 \quad \text{(A32b)}$$

$$e_{zz} = e_3 \quad \text{(A32c)}$$

$$e_{\theta z} = e_4 \quad \text{(A32d)}$$

$$e_{rz} = e_5 \quad \text{(A32e)}$$

$$e_{r\theta} = e_6 \quad \text{(A32f)}$$

with

$$\sigma_1 = C_{11}e_1 + C_{12}e_2 + C_{13}e_3 \quad \text{(A33a)}$$

$$\sigma_2 = C_{12}e_1 + C_{11}e_2 + C_{13}e_3 \quad \text{(A33b)}$$

$$\sigma_3 = C_{13}e_1 + C_{13}e_2 + C_{33}e_3 \quad \text{(A33c)}$$

$$\sigma_4 = C_{44}e_4 \quad \text{(A33d)}$$

$$\sigma_5 = C_{44}e_5 \quad \text{(A33e)}$$

$$\sigma_6 = \frac{1}{2}(C_{11} - C_{12})e_6 \quad \text{(A33f)}$$

and

$$e_1 = \frac{\sigma_1 - \nu_{12}\sigma_2}{E_T} - \frac{\nu_{13}\sigma_3}{E_L} \quad \text{(A34a)}$$

$$e_2 = \frac{-\nu_{12}\sigma_1 + \sigma_2}{E_T} - \frac{\nu_{13}\sigma_3}{E_L} \quad \text{(A34b)}$$

$$e_3 = \frac{-\nu_{13}\sigma_1 - \nu_{13}\sigma_2 + \sigma_3}{E_L} \quad \text{(A34c)}$$

$$e_4 = \frac{\sigma_4}{G_L} \quad \text{(A34d)}$$

$$e_5 = \frac{\sigma_5}{G_L} \quad \text{(A34e)}$$

$$e_6 = \frac{2(1+\nu_{12})\sigma_6}{E_T} \quad \text{(A34f)}$$

Clearly

$$C_{44} = G_L \quad \text{(A35)}$$

and

$$\begin{bmatrix}\sigma_1\\ \sigma_2\\ \sigma_3\end{bmatrix} = \begin{bmatrix}C_{11} & C_{12} & C_{13}\\ C_{12} & C_{11} & C_{13}\\ C_{13} & C_{13} & C_{33}\end{bmatrix}\begin{bmatrix}e_1\\ e_2\\ e_3\end{bmatrix} = B\begin{bmatrix}e_1\\ e_2\\ e_3\end{bmatrix} \quad \text{(A36)}$$

$$\begin{bmatrix}e_1\\ e_2\\ e_3\end{bmatrix} = \begin{bmatrix}1/E_T & -\nu_{12}/E_T & -\nu_{13}/E_L\\ -\nu_{12}/E_T & 1/E_T & -\nu_{13}/E_L\\ -\nu_{13}/E_L & -\nu_{13}/E_L & 1/E_L\end{bmatrix}\begin{bmatrix}\sigma_1\\ \sigma_2\\ \sigma_3\end{bmatrix} = A\begin{bmatrix}\sigma_1\\ \sigma_2\\ \sigma_3\end{bmatrix} \quad \text{(A37)}$$

Hence

$$B = A^{-1} \quad \text{(A38)}$$

$$\det(A) = \frac{1}{E_L}\left[\frac{1}{E_T^2} - \frac{\nu_{13}^2}{E_L E_T} + \frac{\nu_{12}}{E_T}\left(-\frac{\nu_{12}}{E_T} - \frac{\nu_{13}^2}{E_L}\right) - \frac{\nu_{13}}{E_L}\left(\frac{\nu_{12}\nu_{13} + \nu_{13}}{E_T}\right)\right]$$

$$= \frac{1}{E_T E_L^2}\left[\left(1 - \frac{\nu_{13}^2 E_T}{E_L}\right)^2 - \left(\nu_{12} + \frac{\nu_{13}^2 E_T}{E_L}\right)^2\right]$$

$$= \frac{k}{E_T E_L^2} \quad \text{(A39)}$$

where

$$k = \left(1 - \frac{\nu_{13}^2 E_T}{E_L}\right)^2 - \left(\nu_{12} + \frac{\nu_{13}^2 E_T}{E_L}\right)^2 \quad \text{(A40)}$$

So

$$B = A^{-1} = \frac{E_L E_T^2}{k}\begin{pmatrix} \frac{1}{E_T E_L} - \frac{\nu_{13}^2}{E_L^2} & \frac{\nu_{12}}{E_T E_L} + \frac{\nu_{13}^2}{E_T^2} & \frac{\nu_{12}\nu_{13} + \nu_{13}}{E_T E_L} \\ \frac{\nu_{12}}{E_T E_L} + \frac{\nu_{13}^2}{E_T^2} & \frac{1}{E_T E_L} - \frac{\nu_{13}^2}{E_L^2} & \frac{\nu_{12}\nu_{13} + \nu_{13}}{E_T E_L} \\ \frac{\nu_{12}\nu_{13} + \nu_{13}}{E_T E_L} & \frac{\nu_{12}\nu_{13} + \nu_{13}}{E_T E_L} & \frac{1 - \nu_{12}^2}{E_T^2} \end{pmatrix} \quad \text{(A41)}$$

and thus

$$C_{11} = \frac{E_T}{E_L}\left(\frac{E_L - E_T\nu_{13}^2}{k}\right) \quad \text{(A42a)}$$

$$C_{12} = \frac{E_T}{E_L}\left(\frac{E_L\nu_{12} + E_T\nu_{13}^2}{k}\right) \quad \text{(A42b)}$$

$$C_{13} = E_T\frac{\nu_{13}(1+\nu_{12})}{k} \quad \text{(A42c)}$$

$$C_{33} = E_L\frac{1 - \nu_{12}^2}{k} \quad \text{(A42d)}$$

$$C_{44} = G_L \quad \text{(A42e)}$$

The engineering elastic constants for an isotropic material are

$$E = \text{Young's modulus}$$

$$\nu = \text{Poisson's ratio}$$

$$G = \frac{E}{2(1+\nu)}$$

and Equations A42 simplify to

$$C_{11} = C_{33} = \frac{E(1-\nu^2)}{k} \quad \text{(A43a)}$$

$$C_{12} = C_{13} = \frac{E\nu(1+\nu)}{k} \quad \text{(A43b)}$$

$$C_{44} = \frac{E}{2(1+\nu)} \quad \text{(A43c)}$$

where

$$k = (1 - \nu^2)^2 - (\nu + \nu^2)^2$$
$$= (1 - 2\nu)(1 + \nu)^2 \quad \text{(A44)}$$

References

1. R. L. MEHAN, M. R. JACKSON and M. D. McCONNEL, *J. Mater. Sci.* **18** (1983) 3195.
2. R. R. KIESCHKE, R. E. SOMEKH and T. W. CLYNE, in "Developments in the Science and Technology of Composite Materials", Proceedings of the 3rd European Conference on Composite Materials, Bordeaux, March 1989, edited by A. R. Bunsell, P. Lamicq and A. Massiah (Elsevier, London, 1989) pp. 265–72.
3. R. R. KIESCHKE, C. M. WARWICK and T. W. CLYNE, *Metall. Trans.* **39** (1990) 445.
4. T. ISHIKAWA, K. KOYOMA and S. KOBAYASHI, *J. Compos. Mater.* **12** (1978) 153.
5. D. IESAN, *J. Thermal Stress* **3** (1980) 495.
6. Y. MIKATA and M. TAYA, *J. Compos. Mater.* **19** (1985) 554.
7. J. F. NYE, "Physical properties of crystals – their representation by tensors and matrices" (Clarendon, Oxford, 1985) p. 150 *et seq.*
8. R. R. KIESCHKE, R. E. SOMEKH and T. W. CLYNE, *Acta. Metall. Trans.* **39** (1991) 427.
9. K. M. BROWN, R. W. HENDRICKS and W. D. BREWER, in "Fundamental Relationships between Microstructure and Mechanical Properties of Metal Matrix Composites", edited by P. K. Liaw and M. N. Gungor, TMS Fall Meeting 1989 (TMS-AIME, Warrendale, 1990) pp. 269–286.
10. J. D. ESHELBY, *Proc. Roy. Soc.* **A241** (1957) 376.
11. T. MURA, in "Micromechanics of Defects in Solids" (Martinus Nijhoff, Dordrecht, The Netherlands, 1987).
12. M. TAYA and R. J. ARSENAULT, "Metal Matrix Composites" (Pergamon, New York, 1989).

Received 7 March
and accepted 10 October 1990